Allometric change accompanies opercular shape evolution in Alaskan threespine sticklebacks

Charles B. Kimmel[1,4)], **Windsor E. Aguirre**[2)], **Bonnie Ullmann**[1)], **Mark Currey**[3)] **& William A. Cresko**[3)]

([1] Institute of Neuroscience, University of Oregon, Eugene, OR 97403, USA; [2] Department of Ecology and Evolution, State University of New York, Stony Brook, NY 11794, USA; [3] Center for Ecology and Evolutionary Biology, University of Oregon, Eugene, OR 97403, USA)

(Accepted: 27 December 2007)

Summary

How does development evolve to produce a skeletal element with a new shape? We extend our previous study of morphological evolution and development of the opercle, a large facial bone with favorable attributes for both comparative and development analyses. The opercle becomes prominently reshaped when Alaskan anadromous stickleback fish evolve into resident freshwater lacustrine forms. We use geometric morphometrics to examine the opercle shape change which includes a prominent dilation of the bone along one axis, coupled with diminution along the orthogonal axis. During juvenile to adult development, the opercles of both the ancestral and derived forms change in shape as they grow in size, and the allometries differ between the two forms. Hence, a feature of morphological evolution in this system is the appearance of a novel shape–size developmental trajectory in the lacustrine fish. We include a model explaining the ancestral allometric pattern of bone growth, and how growth must be reorganized to bring about the evolutionary change in shape.

Keywords: skeletal morphology, craniofacial patterning, opercle, allometry, heterochrony, heterotopy.

Introduction

The skeleton, more than any other phenotypic feature, provides phylogenetic links among the vertebrates, revealing the course of their evolution. This is

[4)] Corresponding author's e-mail address: kimmel@uoneuro.uoregon.edu

because a large number of these links come from fossils of extinct animals, and their skeletons provide the fossils. Because of the basic supportive and protective roles of the skeleton, we can understand in broad terms how different bone morphologies might be adaptive in different environments and for different life history traits and, hence, how natural selection might influence evolution of these different morphologies. In contrast, we have not yet reached broad understanding of how skeletal morphology arises in the developing organism, or of what basic processes, in terms of gene functions and cellular activities, change during morphological evolution.

Beginning with Haeckel and continuing into more modern times (review; Gould, 1977) theory has addressed the broad nature of developmental change. A different time course, or rate of development between an ancestor and a descendent, may be the critical determinant of morphological change, as proposed in theories based on heterochrony. Alternatively, change in position (heterotopy), size (heterometry), or biochemical/histochemical nature (heterotypy) of features of a primordium might be key (Arthur, 2000, 2004). Among these broad types of developmental change, heterochrony certainly has been the most widely addressed, and has been proposed to underlie many cases of morphological change, including skeletal change (Gould, 1977; Alberch et al., 1979; McKinney & McNamara, 1991; Raff, 1996; Klingenberg, 1998; Schlichting & Pigliucci, 1998; Zelditch, 2001). Yet, even deciding among these broad categories is often not a simple matter, because of the complexities of development and of morphology itself (e.g., Guralnick & Kurplus, 2001).

Allometries, meaning size-shape covariances, are at the heart of morphological change, and lend prominently to its complexity. Skeletal allometries accompany both evolutionary change ('phyletic' allometries) and developmental change ('developmental' or 'growth' allometries). Further, developmental allometries might themselves evolve, as we show here. Such allometry evolution might be underlain by one or other of the broad classes of developmental change outlined above. For example, consider a case in which there occurs in a descendant, a new (i.e., different from the ancestor) coupling in the rates of size and shape change during development, i.e., a type of heterochrony (Alberch et al., 1979). If one could compare the adult morphologies of both ancestor and descendant, this new coupling could be revealed as a change in phyletic allometry. The different couplings would

also be apparent as a change in developmental allometry, if one could examine development of both forms.

However, observing such evolutionary change in allometry as just described does not necessarily signal a heterochronic developmental change. Change in position rather than timing (heterotopy vs. heterochrony) could underlie allometry evolution. As has been emphasized previously (Zelditch et al., 2000), heterotopy has often been ignored in studies where it might have been prominently discussed.

To learn how development changes during skeletal evolution we study the threespine stickleback, *Gasterosteus aculeatus*, a 'model' organism in which investigations of evolution, development, genetics and genomics are all possible (Bell & Foster, 1994; McKinnon & Rundle, 2002; Peichel, 2005; Cresko et al., 2007). Ancestral stickleback are oceanic, and they have frequently, and apparently independently, invaded many freshwater habitats, often undergoing prominent evolutionary change in the process. Reductions in skeletal armor nearly invariably characterize the derived populations. Skeletal changes have evolved repeatedly, in parallel, during the last 10 Myr (Bell & Foster, 1994; Schluter, 2000), and can occur very rapidly (Bell et al., 2004). Furthermore, recent research emphasizes that these separate, but similar evolutionary transitions can involve common genetic machinery (Cresko et al., 2004; Colosimo et al., 2004, 2005; Shapiro et al., 2004). Crucially for such studies, one can examine, and make genetic crosses between fish from ancestral and descendant populations. Recent progress with this species, including a completely sequenced genome (http://ensembl.genome.tugraz.at/Gasterosteus_aculeatus/index.html), makes understanding the genetic basis of vertebrate morphological evolution possible, and motivates our desire for a fuller understanding of skeletal shape evolution in this system.

To simplify analyses, we examine a single element of the facial skeleton, the opercular bone, or opercle (OP; Figure 1). The OP characteristically provides the main support for the protective gill cover, or operculum, in bony fish (class Osteichythes) and serves important functional demands. Respiration depends on expansion and compression of the opercular chamber (Hughes, 1960), as mediated by inward-outward movement of the gill cover that directly involves a ball-and-socket joint that the OP makes with a deeper facial supportive bone, the hyomandibula. Lifting the operculum towards the dorsum involves the same joint, but uses different muscles. In

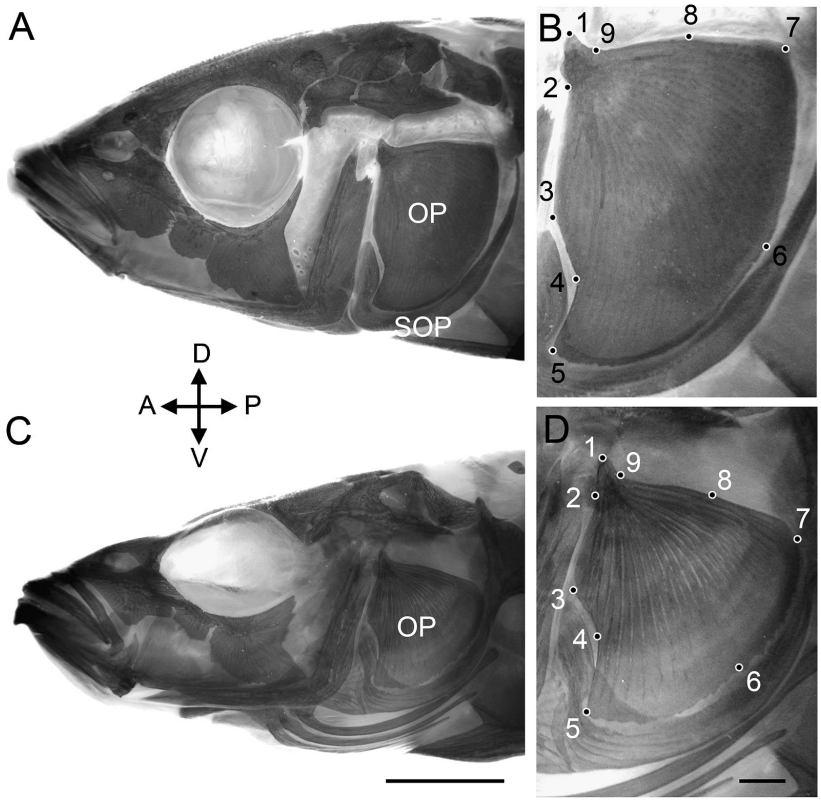

Figure 1. OP shape evolves in AK sticklebacks. Left side facial views of Alizarin Red S stained fish (A, C) and enlargements of the opercular region (B, D). (A, B): Alaskan anadromous fish captured in Mud Lake (SL = 70.5 mm). (C, D): Alaskan resident lacustrine fish captured in Visnaw Lake (SL = 61.9 mm). Landmarks used in the TPS analyses are shown in B and D. Scale bars: 5 mm (A, C), 1 mm (B, D).

many fishes this OP lifting serves as part of a jaw opening mechanism used in feeding, because the OP is functionally connected through a series of ligaments and bones to the lower jaw (Anker, 1974; Lauder, 1979; Lauder & Liem, 1983). As one then might expect from these considerations, quite a striking diversity of OPs has evolved among the osteichthyans.

Furthermore, the OP has favorable attributes for developmental genetic study (for review, Kimmel et al., 2007). The OP is one of the first bones to arise during development, around the time of hatching in sticklebacks (about 7 days post-fertilization). It develops key features of its shape within a time frame of hours and days. Because of its superficial location, just beneath the

skin, it is directly visible during early development in the living, intact preparation. Mutational analyses in zebrafish provide insight into genetic pathways important for its shaping and sizing (Kimmel et al., 2003; Miller et al., 2007). Moreover, we discovered that in freshwater Alaskan populations of threespine stickleback, the OP has evolved a markedly derived form from its ancestral shape. The change is genetically based, and can be detected in young larvae, as well as in adults (Kimmel et al., 2005). These findings provide the foundation for the current study.

Previously, we estimated the evolutionary reshaping of the OP using linear measurements between the three apices of the approximately triangular shaped bone (Figure 1B, D; landmarks 1, 5 and 7). These lengths of the triangle sides were different, and not all in proportion, between the anadromous and lacustrine fish, allowing us to infer how the bone shapes differed. However, the method did not completely capture nuanced but important changes in opercle shape, and only partially separated shape changes from changes in size (i.e., scaling). Here we extend our analysis by using more powerful procedures of geometric morphometrics, including thin plate spline (TPS) transformation (Rohlf, 1998; reviewed by Zelditch et al., 2004). A particular advantage of the method is that shape can be examined uncontaminated by size effects (with, of course, the notable exception where shape and size covary due to allometry). With these new multivariate analyses, we significantly extend and revise our understanding of the nature of the evolutionary change in opercle morphology. We find that the prominent shape change is a coupled dilation–diminution; the bone stretches out along one axis and shrinks along the orthogonal axis. Finally, we propose a model explaining a likely basis for the difference in developmental allometries.

Material and methods

Stickleback collections

Most adult Alaskan (AK) threespine stickleback (*Gasterosteus aculeatus*), initially wild-captured, came from collections from one of us (WAC) at the University of Oregon (anadromous fish from Anchor River and Rabbit Slough, lacustrine fish from Mud Lake; Cresko et al., 2004; Kimmel et al., 2005). Adults from Mud and Visnaw Lakes (Caldecutt & Adams, 1998) were provided by M.A. Bell, State University of New York at Stony Brook (Stony

Brook, NY, USA). Boot Lake (lacustrine) and Rabbit Slough (anadromous) fish were reared in the laboratory (Cresko et al., 2004), providing for controlled studies of the two forms developing under standardized and uniform conditions.

Data collection and analysis

Stickleback were fixed in 10% formalin, stored in 50% isopropanol and then stained with 1% Alizarin Red S. We measured the body sizes as standard lengths (SL) and photographed left side head views of the animal in the sagittal plane, as in Figure 1, carefully attempting to keep to standard orientation. To carry out the TPS analyses we used the 'tps' software package from the State University of New York at Stony Brook, digitizing the positions of the nine landmarks shown in Figure 1C and D (tps Dig version 2.04 software; Rohlf, 2005a). Four of these landmarks (Nos. 3, 4, 6, 8) were treated as sliding semi-landmarks (Bookstein, 1997; for review, see Zelditch et al., 2004). Landmarks 1, 2 and 9 capture detail around the joint region of the bone, where it connects with the hyomandibula. Semi-landmarks 3 and 4 show the contours of a prominent indented region along the OP's anterior edge, where it conjoins a neighboring bone, the subopercular. Semi-landmarks 6 and 8 are approximately at the middles of the other two edges.

Using the entire data set ($N = 231$), we aligned the configurations by Procrustes generalized least squares superimposition, removing size, rotation, and translation effects. We saved the aligned data (OP 'shape coordinates'; for review, see Zelditch et al., 2004), centroid sizes (CS), a single consensus configuration (shown below, Figure 4B), the set of shape variables (partial warp scores), and the set of ten principal component (PC) scores (also termed relative warp scores) from each configuration (tps Relative warps version 1.42 software; Rohlf, 2005c). Subsets of the aligned configurations were averaged in order to compare TPS deformations (e.g., as in Figures 3 and 5, tps Thin-plate spline version 1.20 software; Rohlf, 2004). Multivariate regression analyses and MANCOVA were carried out with a subset of the data with tpsRegr, version 1.31 (Rohlf, 2005b). For the regression analysis we included only lab-reared juvenile and adult fish from Boot Lake (lacustrine) and Rabbit Slough (anadromous). ANOVA and other statistical analyses were carried out with JMP version 5.1 software (SAS Institute, Cary, NC, USA). Discriminant function analysis was also carried out with SPSS

11.0.0 (SPSS, 2001) to assess levels of population differentiation. These tests utilized a leave-one-out classification procedure, such that each case in the analysis is classified by the functions derived from all cases other than that case.

Results

Opercular shape evolution in Alaskan sticklebacks includes a characteristic set of regional deformations of the bone

Discriminant function analysis, based on the shape variables, the partial warp scores, revealed no misclassifications among anadromous versus lacustrine individuals, regardless of whether the specimens were wild-caught or raised in the laboratory (Figure 2). In a second, more stringent test, a single individual was misclassified. The wild-collected lacustrine populations from Mud Lake and Visnaw Lake shown in Figure 2A are also clearly distinct from one another, but a few fish were misclassified in either the standard or more stringent method (details and statistics in the figure legend). Procrustes distances, giving single measures of the shape disparities, support the interpretation that the OP shape deformations between the two lakes are less prominent than the deformation between the anadromous form and either lake. The Procrustes distances between the anadromous and the two lacustrine populations in Figure 2A are similar in magnitude (0.10 for Mud Lake and 0.12 for Visnaw), whereas the Procrustes distance between the two lacustrine configurations is only 0.03.

The shape transformation between the anadromous and lacustrine form involves stretching or compressing local regions of the bone, as we illustrate for lab-reared anadromous (Rabbit Slough) and lacustrine (Boot Lake) adult fish in Figure 3A and B. One area of the reference grid in the upper part of Figure 3B, made by thin plate spline (TPS) transformation, is pulled out and another pushed in, in the manner shown by D'arcy Thompson's (1942) famous deformation grids. Importantly, and invisible in our previous analysis (Kimmel et al., 2005), regional deformations spanning several landmarks occur, as illustrated by vector plots (Figure 3B, lower). For example, landmarks 9, 1, 2 and 3 all move together in roughly the same direction in the deformation. Deformations made from lacustrine versus anadromous wild-collected fish (not shown), or from juvenile lab-reared fish (see below, Figure 5C and F) are broadly similar to the one illustrated, suggesting that the

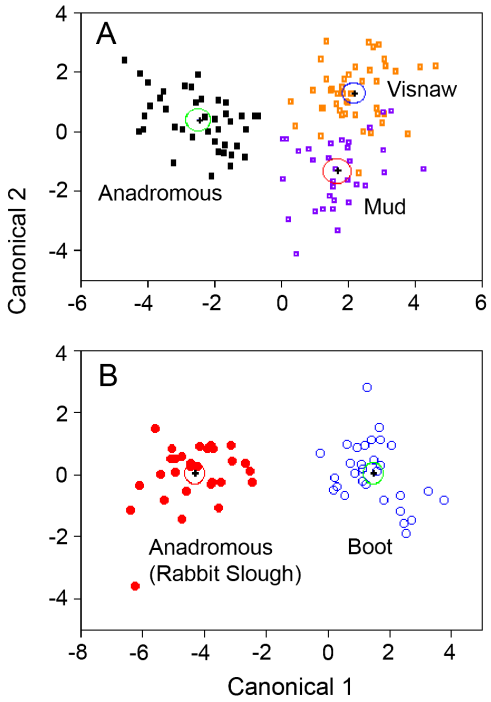

Figure 2. Discriminant function analysis distinguishes adult stickleback populations with only few errors. The analyses are based on the partial warp scores, serving as OP shape variables. The canonical plots show the distributions of the individual adult specimens and include the population means as cross-hairs, and 95% ellipses for the groups. The analysis assigns, without error, individual specimens as anadromous or lacustrine, whether wild-captured (A) or lab-reared (B). (A) $N = 40$ anadromous, solid rectangles, 30 from Mud Lake, small open squares, and 41 from Visnaw Lake, open rectangles Wilks' $\lambda = 0.084$, $\chi^2_{[20]} = 266.875$, $p < 0.001$. (B) $N = 30$ anadromous (originating from Rabbit Slough, closed circles) and 30 originating from Boot Lake (open circles) Wilks' $\lambda = 0.104$, $\chi^2_{[10]} = 115.558$, $p < 0.001$. In an alternative, more stringent leave-one-out classification test, one Mud Lake resident collected as an adult directly from the wild was misclassified as an anadromous specimen. The discriminant analysis also mostly correctly distinguishes between the wild-captured resident fish from Mud Lake and Visnaw Lake in panel A. In this case, in the standard analysis three Mud Lake specimens were misidentified as originating from Visnaw Lake, and three Visnaw Lake specimens were misidentified as originating from Mud Lake (the more stringent leave-one-out classification test resulted in a total of eight misclassifications between the two lacustrine groups). This figure is published in colour at http://www.ingenta.com

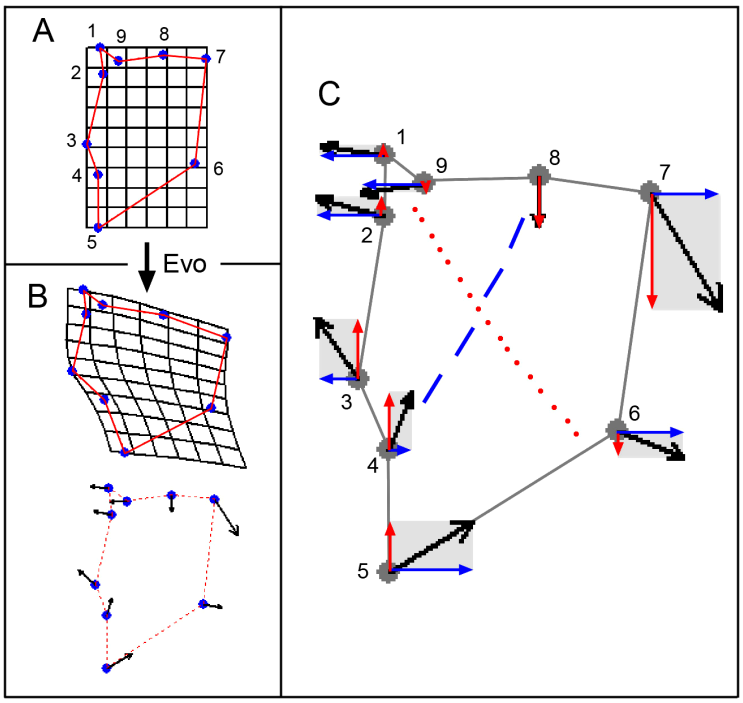

Figure 3. Dilation–diminution characterizes OP shape evolution. (A) The landmark configuration of averaged lab-reared Rabbit Slough adults, serving as a reference for B, the deformation accompanying evolution to the lacustrine form, averaged lab-reared Boot Lake adults, shown as a TPS deformation (top, ×2) and as vector displacements along the configuration (bottom, ×2). (C) Vector displacements resolved into displacements of the x- and y-coordinates. Average vector displacements (×4) averaged from all the lacustrine fish in the study set (not just the lab-reared fish); the reference is the average of all of the anadromous fish (wild, lab-reared, adults and juvenile). The mean difference in displacement for each x- and y-coordinate, between anadromous and lacustrine fish, is significant ($p < 0.0001$, ANOVA), except for X8 ($p = 0.44$) and Y9 ($p = 0.01$). This figure is published in colour at http://www.ingenta.com

change we see in Figure 3B is predominantly associated with evolution from the oceanic to the lacustrine condition, and not simply due to chance or to some local peculiarities of the individual lacustrine environments, or, as we explore further below, to OP size differences.

To analyze these landmark displacements in greater detail, we compared the averaged configurations from lacustrine and anadromous fish within our entire data set (i.e., all populations, including lab-reared juveniles), generating the vector plot of the anadromous to lake deformation shown in Fig-

ure 3C. This deformation, here magnified 4 times, is again quite similar to that in Figure 3B. The displacements at or near the OP joint region, to the upper left side of the configuration (landmarks 9, 1, 2, 3), all show a significant negative x-displacements (Figure 3C; see legend for statistics), whereas the displacements on the lower right side, along the ventral-posterior edge of the bone (landmarks 5, 6, 7) show significant and prominent positive x-displacements. The combined effect of the changes in the two regions, negative on the left side and positive on the right side, is to produce a prominent stretching, or dilation, of the configuration along roughly the x-axis (corresponding to the anterior-posterior axis of the body of the fish; Figure 1). A 'null zone' with respect to x-coordinate displacement is present between these two regions showing opposite sign, at landmarks 4 and 8, and we show this zone by the dashed line across the configuration in Figure 3C. At landmarks 4 and 8, the x-coordinate displacement is small (and insignificant in the case of landmark 8).

In a manner similar to these changes along the x-axis, the y-coordinate displacements in the lower left part of the configuration are opposite in sign to those in the upper right part; the dotted line running from the joint region, defined by landmarks 9, 1 and 2, to landmark 6 separates these two areas (Figure 3C). In this case, the combined effect of the upper and lower displacements compresses the configuration, roughly along the y-axis (or dorsal-ventral body axis).

In summary, as revealed by multivariate landmark analyses, the evolutionary shape change of the lacustrine OP includes prominent and stereotyped broad regional deformations, dilation along one axis of the bone, and diminution along a roughly orthogonal axis. We also note a local change along the anterior-ventral edge of the bone captured by landmarks 3 and 4, and shown particularly well by the TPS transformation in Figure 3B; an indented region of the anadromous form becomes yet more indented in the lacustrine form. As shown in Figure 1, this indentation occurs where the OP joins with the dorsal part of the neighbouring subopercular bone (SOP).

Covariances in the landmark displacements

We carried out principal component analysis (PCA) to capture the pattern of variances and covariances associated with OP shape evolution, and to help us understand developmental correlates, as we describe below. Using the Procrustes-aligned landmark configurations from our entire data set

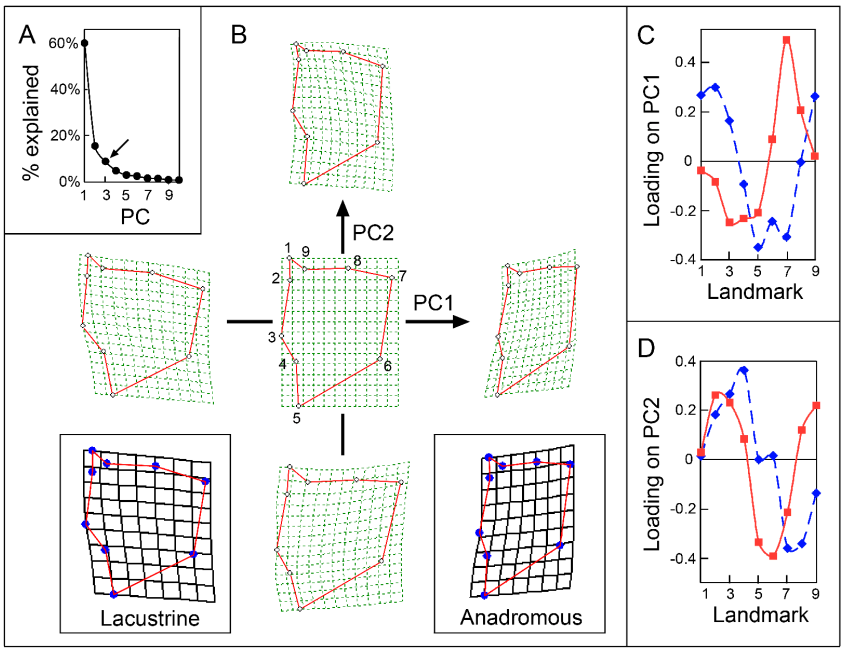

Figure 4. Principal component analysis of OP shape evolution. (A) Scree plot showing cumulative percent variance explained by the 11 PCs obtained from aligned landmarks for all of the samples ($N = 231$) in the data set. PC1 explains 60%, PC2 16%, and PC3 9% of the variance. These first three PCs, collectively capturing 84% of the total variance, are above a prominent inflection on the curve (arrow) and, therefore, are most likely to contain important biological information (Zelditch et al., 2004). (B) TPS deformations associated with changes in PC1 (horizontal axis) and PC2 (vertical axis), with the overall consensus configuration at the center. The boxed insets show that OP shape evolution from the anadromous to lacustrine form resembles the change the negative direction along PC1. The two boxed TPS deformations are AK adult lacustrine and adult anadromous, and for each form, the separate populations, including lab-reared or wild-captured fish, are pooled). We obtained both deformations with the consensus configuration for the entire data set (center in B) as the reference. (C) Loadings of the landmark displacements (eigenvectors) on PC1 and PC2. These plots can be compared with the vector plot in Figure 3B, revealing that generally the displacements of large positive or negative magnitude, show correspondingly high loadings on the PCs. This figure is published in colour at http://www.ingenta.com

($N = 231$), we obtained 10 principal components (PCs). Examining a scree plot of the variance explained by each PC indicates that the first three may contain relevant biological information (Figure 4A; Zelditch et al., 2004). We used these three PCs, collectively capturing 84% of the total shape variance, for all subsequent quantitative shape analyses, although in fact PC1

and PC2 yielded the more useful information. Figure 4B shows the consensus landmark configuration in the center, and how the configuration deforms along both the PC1 and PC2 axes. The boxed insets in Figure 4B compare the average deformations of the anadromous and lacustrine forms relative to this same consensus configuration. It is evident from the figure that PC1 itself largely captures the evolutionary change in shape. Because of this observation we focus our attention on PC1 in particular for characterization and quantification the evolutionary change in shape.

How the landmarks load onto the PCs is also revealing about the nature of covariances associated with the evolutionary change in shape (Figure 4C, D). In particular, the PC1 loadings closely match, across the entire landmark configuration, the magnitudes of the landmark displacements described above (Figure 3C). Thus, for example, coordinate Y7 shows a large displacement between anadromous and lacustrine fish (Figure 3C), and correspondingly, Y7 loads heavily on PC1 (Figure 4C).

Developmental allometry: size–shape covariance

To begin to understand the evolutionary changes in developmental mechanisms that produce the morphological differences we observe at the adult stage just described, we examined a series of staged juvenile and young adult Rabbit Slough and Boot Lake fish, reared in the laboratory. We note the prominent markings, defined by sites of dense alizarin red staining, on the surfaces of the young OPs (Figure 5A, B, D, E). These markings include rays radiating out from the joint region, defined by the 9, 1, 2 set of landmarks, toward the opposite edge of the bone, defined by landmarks 5, 6 and 7. In addition to these rays, bands are present that are oriented roughly orthogonal to the rays, and parallel to the 5, 6, 7 edge. Together, the rays and bands give the bone surface a characteristic lattice-like appearance.

The juvenile (mean SL = 19 mm, CS = 2.1, 42–44 days post-fertilization), and youngest adult (SL 28 mm, CS = 3.1, 72–76 days post-fertilization) lacustrine and anadromous OPs are already distinctive in shape (in fact differences are already present in the newly hatched larva; Kimmel et al., 2005). The landmark deformations between lacustrine and anadromous fish at the stages shown are broadly similar to the deformations at the fully adult stage (Figure 5C, F, compare with Figure 3B). Development between the two stages shown in Figure 5 includes considerable increase in size in both forms

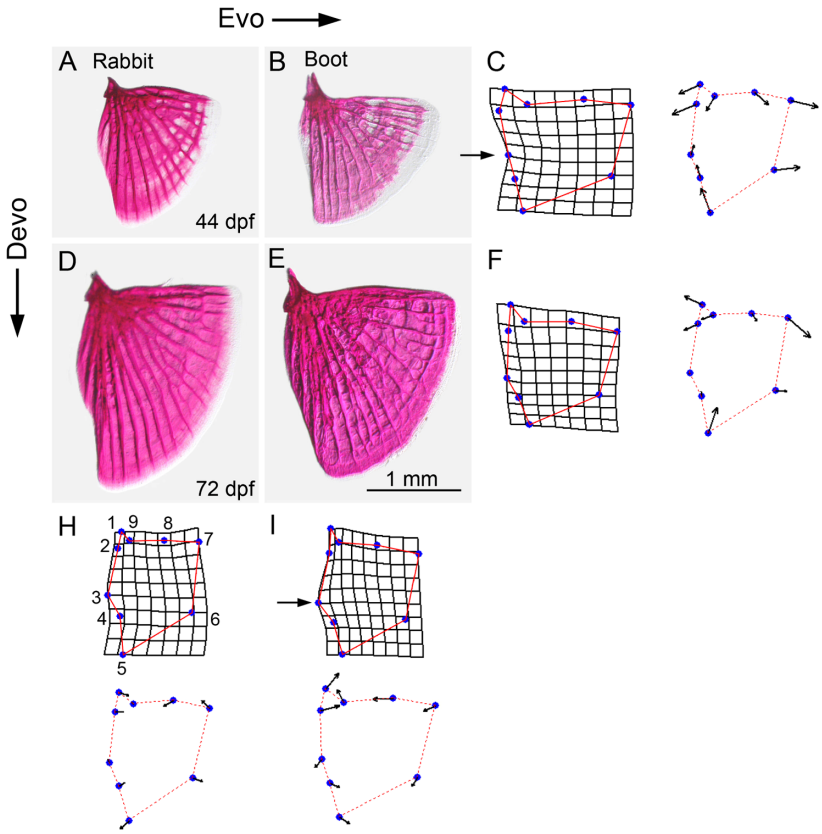

Figure 5. Morphological change in the OPs of anadromous and lacustrine fish developing in the laboratory. Two stages are shown, a young juvenile stage (A–C, 42–44 days post-fertilization (dpf), mean centroid size = 2.1, $N = 12$) and a young adult stage (D–F, 72–76 dpf, centroid size = 3.1, $N = 13$), in both the anadromous (A, D, H) and lacustrine (B, E, I) forms. Centroid size varies approximately as the log of days postfertilization during this interval of development, and extending out to the fully mature forms (data not shown). The photographs (A, B, D, E) show Alizarin Red-stained OPs, isolated by dissection after fixation and staining. Note the prominent markings indicating regions of higher dye uptake. Rays radiate out from the joint region (marked by landmarks 9, 2, 1; upper left) and curved bands, that we can identify as incremental growth bands, lie in parallel the opposite edge of the bone (the edge marked by landmarks 5, 6, 7; to the lower right). C and F show the evolutionary deformation at the two stages, with the appropriate anadromous form (Rabbit Slough) serving as the reference for the lacustrine deformation (Boot Lake). H and I show developmental deformations for both forms between the two stages, with the younger stage serving as the reference for the older. The arrows pointing out displacements at landmark 3 in F and I, and exemplify the complementary nature of the deformations associated with evolution and development: the evolutionary deformation is inward and the developmental one outward. This figure is published in colour at http://www.ingenta.com

(Figure 5D vs. A, and E vs. B), and noticeable reshaping (Figure 6H, I). The TPS deformations of lacustrine and lake OPs are broadly similar, for example both include an outward bulge at landmark 3 (arrow, Figure 5I). However, shape deformations along the evolutionary (Figure 5C, F) and developmental (Figure 5H, I) trajectories are dissimilar; we note that in many respects they appear opposite in sign to one another (e.g., at the inward budge at landmark 3, arrow in Figure 5F). A prominent apparent difference is that the evolutionary change noticeably broadens both young and older configuration along the horizontal axis (the x-axis as described above), and the developmental change narrows both lacustrine and anadromous configurations along the same axis.

Our data suggest that as the OP grows in size in both lab-reared anadromous and lab-reared lacustrine fish it also changes in shape, i.e., that development is allometric (Figure 5H, I). We used multivariate regression analysis, in which the partial warps, shape variables including the uniform component, are regressed on centroid size, the size variable, to test whether allometries are in fact present. This analysis revealed that significant allometries characterize OP development for both forms (anadromous, Wilks' $\lambda = 0.1594$, permutation test, $p < 0.001$; lacustrine, Wilks' $\lambda = 0.0609$, permutation test, $p < 0.001$). Furthermore MANCOVA reveals the allometric slopes for the two forms are distinct (Wilks' $\lambda = 0.0270$, permutation test, $p < 0.001$), meaning that the ancestral allometry characterizing the anadromous fish has evolved to a new pattern in the derived, lacustrine fish.

The same relationships are also reflected in regressions based on our Principal Components Analysis. PC1 exhibits two distinct regression lines for the anadromous and lacustrine fish, when regressed on centroid size (Figure 6A, see legend for all associated statistics). The slope of the line for the anadromous fish is positive and differs significantly from zero. The slope of the line for the lacustrine fish does not differ significantly from zero (the condition for isometry), but ANCOVA shows that the slopes of the anadromous and lacustrine lines differ significantly from one another. We interpret this difference to mean that an evolutionary change has occurred in the allometry underlying the prominent aspects of OP shape captured by PC1.

The change in slope for the lacustrine fish (Figure 6A) is, itself, consistent with shape development occurring isometrically in these derived fish (i.e., size increase without shape change), as if evolution has 'turned off' OP developmental shape allometry. However, as pointed out above, thin-plate

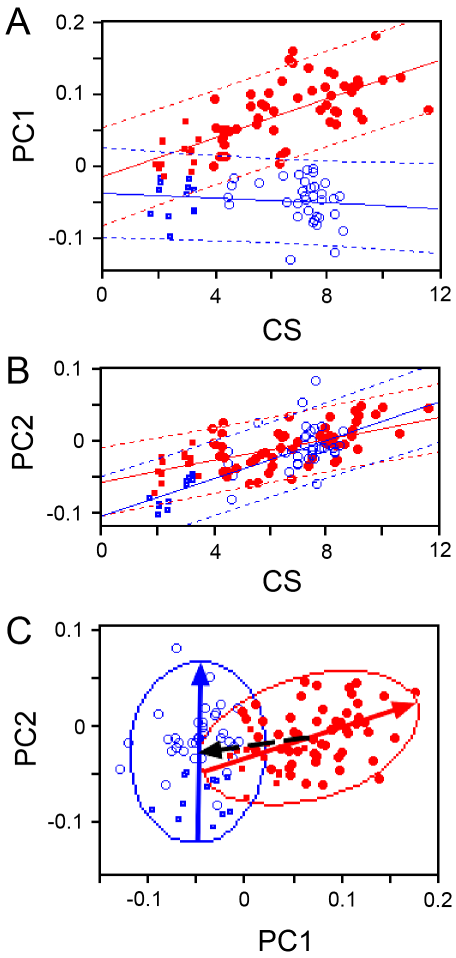

Figure 6. Different allometries characterize OP shape development trajectories in anadromous and lacustrine sticklebacks. Open symbols: lab-reared lacustrine juveniles (small open rectangles and adults (large open circles) originating from Boot Lake. Filled symbols: lab-reared anadromous juveniles (small filled rectangles) and adults (large filled circles) originating from Rabbit Slough. (A, B) Covariances between principal components describing OP shape (PC1 in A and PC2 in B) and size (centroid size, CS). The dashed lines show 95% confidence intervals. The two slopes in both A and B are significantly different from one another, as shown by testing for homogeneity of slopes, (A) $F_{1,110} = 34.8$, $p < 0.0001$; (B) $F_{1,110} = 8.6$, $p = 0.004$. (C) Trajectories (vectors) and 95% ellipses for the same specimens though a PC1×PC2 shape space. The vertical (lacustrine) and nearly horizontal (anadromous) arrows, along the long axes of the 95% ellipses for these populations, show developmental trajectories. The dashed arrow, from the mean of the anadromous set to the mean of the lacustrine set, shows the evolutionary trajectory. This figure is published in colour at http://www.ingenta.com

spline analysis showed a shape difference in OPs from lacustine fish of different stages (Figure 5I), directly suggesting that allometry is present in the lacustrine form (Figure 5I), and multivariate regression verified that shape and size both change during lacustrine OP development. We resolve the apparent paradox by considering PC2, an axis orthogonal to PC1 through shape space. Regression of PC2 on CS (Figure 6B, also PC3, not shown) does indeed reveal significant allometry for lacustrine OP development along this axis. In this case the slope of the lacustrine regression line is significantly larger than that of the anadromous regression line (ANCOVA, see Figure 6 legend).

Thus, our data suggest that in the evolutionarily derived lacustrine fish, allometry has been reduced along one multivariate axis (PC1) and increased along a second (orthogonal) axis (PC2). The putative redirection in developmental allometries revealed by these plots is illustrated most clearly by comparing developmental trajectories of the two forms, lacustrine and anadromous, through a bivariate PC1 by PC2 shape space (Figure 6C). The two forms occupy largely separate neighborhoods of this space (the data points for the two groups are mostly nonoverlapping). Prominent OP shape change of lacustrine fish developing from early juveniles through adults occurs along PC2 (the vertical arrow, or vector, in Figure 6C), whereas the shape change for anadromous fish, while including a PC2 component, occurs predominantly along PC1 (more horizontal solid arrow), nearly opposite in direction to the evolutionary change between anadromous and lake fish (approximated by the dashed arrow).

Discussion

Here we report multivariate analyses of morphological evolution and development of the opercle, a large, early developing facial bone in Alaskan threespine stickleback. We find, in agreement with our earlier work, prominent reshaping of the OP when anadromous stickleback evolve into lacustrine forms. OP shape differences are also present between two lake populations of stickleback, but are more modest in scale. As demonstrated in our studies of lab-reared juvenile and adult fish, OP development is allometric; OP size and shape co-vary. However, the covariance is distinctive for the two forms, suggesting that evolution has modified the ancestral trajectory of allometric growth.

Opercle shape evolution

The TPS landmark configuration deformations nicely capture both evolutionary and developmental changes in OP shape. Our discriminant function analysis reveals that both wild-captured and laboratory-reared adults show OP shape differences that are similar in nature and magnitude, confirming our earlier finding that a major part of the change is due to genetic, rather than environmental differences. The deformations are similar for adults and juveniles in laboratory-reared fish. The largest landmark displacements in both comparisons (Figures 3 and 5) occur at the ventral and posterior apices of the roughly triangular-shaped bones at landmarks 5 and 7. Other local deformations are present along the edges and, in the PCA, a number of these changes are associated with a single principal component, PC1, that explains 60% of the shape variance. The shape deformation accounted for by PC1 is essentially the same deformation that occurs between the anadromous and lacustrine fish (Figure 4B). Therefore, change along a single multivariate axis, PC1, largely describes evolution in this system, facilitating our ability to understand it and to further analyze it.

The wild-captured fish we examined from Mud and Visnaw lakes differ less in OP shape than do the anadromous and lacustrine stickleback we studied. We selected these two lakes because their stickleback have well-described morphometric differences associated with a putative trophic difference (Walker, 1997; Walker & Bell, 2000; see also Caldecutt & Adams, 1998), and because facial forms for the same populations have already been described (Caldecutt & Adams, 1998). The body shape of the Mud Lake population is benthic, characteristic of fish that feed along the bottom. The Visnaw population has body shape characteristics of limnetic, surface feeding fish. The Caldecutt & Adams morphometric study of face shapes of fish from these lakes, compared with anadromous fish from Rabbit Slough (the principal anadromous population that we use as well), showed prominent differences. A conclusion from that study was that the anadromous condition was intermediate between the two lakes, and somewhat more resembled Visnaw than Mud populations. This is quite different from our findings for the OP, even though our populations come from the same localities, and three of the landmarks used in the two studies (the landmarks at the OP apices) are identical. Assuming both studies are valid, one must conclude that OP shape covaries little or not at all with other prominent features of facial shape in these fish. The question may be worth exploring in greater detail in the future.

Toward a cell-biological explanation of the evolutionary shape change

A promise of the recent developmental and genetic work in stickleback, and in particular, the advances in stickleback genomics, is that we are approaching an understanding of evolutionary change in terms of molecular genetics. Recent studies in stickleback have pointed to major-effect developmental regulatory genes, *Eda* and *Pitx1*, as the critical mediators of evolutionary armor loss (Shapiro et al., 2004; Colosimo et al., 2005). Changes in developmental regulatory genes might more generally be key effectors of morphological evolution. Previously, we noted that genes in the Endothelin1 pathway are candidates for OP evolutionary changes (Kimmel et al., 2005), since this pathway regulates dorsal-ventral patterning of the hyomandibular region of the face in diverse gnathostomes (for review, see Kimmel et al., 2007). In zebrafish, mutations in Edn1-pathway genes affect the shape of the OP (e.g., Miller et al., 2007) in ways that can be reminiscent of the evolutionary change we see in stickleback.

This promise provides part of our motivation for the reanalysis of OP shape presented in this paper. Molecular genetics provides mechanism and insight, and, as we learn more, a blueprint for evolutionary change. However, molecular genetic studies, and documentation of differences at the molecular level between ancestors and descendants, cannot yet directly address changes in the behaviour of developing cells. If we are to understand evolutionary change in bone morphologies, addressing these cell-level changes is critical, for cells build the morphologies. The quantitative phenotypic study of the course of developmental change in bone shape that we provide here is a step toward cell biology.

Evolution changes the ancestral allometries in a way that we did not appreciate in our initial study (Kimmel et al., 2005). Our analysis (particularly as presented in Figure 6C) immediately suggests that the descendent developmental trajectory is novel; i.e., shape development is occurring along a course that is distinctive from that of the ancestor. At essentially any stage along the trajectory, the shape of the descendant bone is novel as well; ancestors and descendants occupy nearly entirely different regions of the space.

This distinctive shape-space occupancy between the ancestral and derived forms puts limits on the plausibility of different kinds of cellular-level changes that might underlie the evolutionary change. A valid model will have to explain the novelty. For the OP to become larger along one axis and shorter

along the other, something new must be occurring within the bone forming primordium itself (Atchley & Hall, 1991). Hence, in accord with our earlier study, our finding does not support a model in which the cells of the primordium all make bone at a new rate, or they all make bone for a longer or shorter period of development. We make this interpretation because, as pointed out by Godfrey & Sutherland (1995) with such heterochronic evolutionary change we expect no deviation from 'ancestral vector pathways'. In other words, if the change were heterochronic in this restricted sense, we would expect the slope of the descendent trajectory through shape space to not differ from the ancestral trajectory. Rather, the trajectory length would change — reflecting a changed duration or rate of shape bone development in the descendant. In contrast, the prominent change we observe is in slope (Figure 6C).

A dilation-diminution model of developmental change

The novelty we have encountered suggests that change within the primordium, perhaps in the number of bone-forming cells (heterometry) and more likely their spatial arrangements (heterotopy) underlies the OP evolutionary change. The heterotopy model seems the simpler to us because a cellular rearrangement can at once explain how bone growth can be diminished in one region and expanded in another (i.e., because cells have relocated from one to the other region). In fact, heterotopy may be generally more important in shape evolution than has been realized in the past (Zelditch et al., 2000). The detailed pattern of change, coupled with what we currently understand about OP growth during larval and juvenile development allows us to formulate a specific model of how development has evolved. OP ossification is initiated at the joint region (marked by landmarks 9, 1 and 2) (Kimmel et al., 2005, 2007), and thereafter the bone grows appositionally, with increments of newly added bone showing up as bands, as in the manner of tree-rings. The incremental bands (Smolyar & Bromage, 2004) are quite visible in our alizarin-stained preparations of young OPs (Figure 5), lying parallel to the ventral-posterior edge, the edge marked by landmarks 5, 6 and 7. Hence we can infer that most bone addition occurs along this ventral-posterior edge. This incremental growth occurs both in the anadromous and lacustrine forms, outward from the joint region as we indicate by the arrows in Figure 7A and C. In the anadromous form, bone growth is markedly asymmetric, occurring at a higher rate ventrally than dorsally.

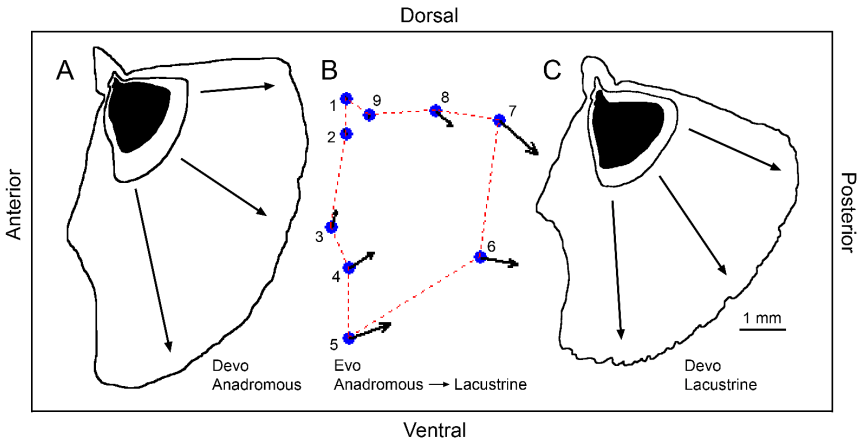

Figure 7. Dilation-diminution model of OP growth and the changes in developmental allometry characterizing the anadromous to lacustrine deformation. (A) Growth and reshaping of the anadromous OP between 42 dpf (centroid size (CS) = 2.1) and 764 dpf (CS = 8.9). The intermediate stage is at 72 dpf, CS = 3.1. A dorsal-ventral gradient characterizes the outward growth (arrows), incrementally along the 5, 6, 7 edge, that starts from the joint region. (B) Vector plot of the anadromous to lacustrine deformation, with reference to the joint region, so as to match A and C, rather than in the usual Procrustes alignment. A replot of the same data as in Figure 3C (scale ×2). The configuration is taken out of the Procrustes alignment, by translating it to the left, along the x-axis (the anterior-posterior axis in Figure 7), such that all negative x-coordinates become zero or positive. This effects a new x-alignment at the joint region. As indicated by the set of vectors, posteriorward bone addition occurring along the 5–6–7 edge is relatively more prominent for the lacustrine form than for the anadromous form (dilation). Coincidently, the dorsal-ventral gradient of bone addition along the same edge is reduced, such that the length of the edge is shortened (diminution). (C) Growth and reshaping of the lacustrine OP between 44 dpf (CS = 2.1) and 666 dpf (CS = 8.3). The intermediate stage is at 76 dpf, CS = 3.1. As a consequence of the evolutionary change, outward incremental growth characterizing the ancestor is increased and the dorsal-ventral gradient is reduced. Scale bar = 1 mm. This figure is published in colour at http://www.ingenta.com

Evolution changes the ancestral pattern in the two ways, as we diagram in Figure 7B. Here we use the landmark configuration we analyzed in detail in the Results (Figure 3C), but with the deformation reconfigured (see Figure 7 legend) to emphasize evolutionary change with reference to the joint region (Figure 7A and C). This presentation clarifies developmental changes in the lacustrine form (Figure 7C) relative to the anadromous form. First, there is greater addition along the 5–6–7 edge, extending this edge further outward (posteriorward) as could be caused by a relatively higher rate of incremental growth along this edge. The change explains the observed dilation

in OP shape along the anterior-posterior axis. Second, evolution reduces the magnitude of the dorsal-ventral gradient of incremental bone addition, such that the same edge of the OP is shortened dorsoventrally, explaining shape diminution along this axis.

A detail not fitting with this dilation-diminution model is the local change along the anterior edge of the OP at landmarks 3 and 4. In particular, the model does not predict the dorsalward deformation at landmark 3 (from the model we expect a mirror image of the change at landmark 8, Figure 7B). The sculpturing here fits the OP to the dorsal part of the SOP, and presumably would tend to optimize the conjoining of the two bones in the derived form. The data in Figure 5 show that the indentation becomes more prominent during late development, both in the anadromous and lacustrine forms. Further study is necessary to determine the pattern of bone growth in this region, and to learn whether interactions between the two developing bones serve to regulate their local shapes.

Our dilation-diminution model provides guidance for further study. It makes clear that one must focus on the behaviour of osteoblasts along the OP posterior-ventral edge. With suitable cellular markers now available in part because of the advances in stickleback genomics, we can examine the appropriate cellular population directly. The elevated rates of incremental addition that we suggest occur during development in the ventral region of this edge of the ancestral OP, and the dorsal region of the descendent OP, might be caused by higher rates of bone deposition by individual osteoblasts, by larger populations of osteoblasts, or by both changes together.

Acknowledgements

We are grateful to Mike Bell for sharing stickleback collections. We thank Dolph Schluter, anonymous reviewers, and our editor Susan A. Foster for constructive comments on earlier drafts. The research was supported by a NSF grant IBN 023639 to John H. Postlethwait, University of Oregon, and NIH grant DE13834 to C.B.K. Support for Windsor E. Aguirre by the W. Burghardt Turner Fellowship program and the Alliance for Graduate Education and the Professoriate (SUNY, Stony Brook) is gratefully acknowledged.

References

Alberch, P., Gould, S.J., Oster, G.F. & Wake, D.B. (1979). Size and shape in ontogeny and phylogeny. — Paleobiology 5: 296-317.

Anker, G.Ch. (1974). Morphology and kinetics of the head of the stickleback, *Gasterosteus aculeatus*. — Trans Zool. Soc. Lond. 32: 311-416.

Arthur, W. (2000). The concept of developmental reprogramming and the quest for an inclusive theory of evolutionary mechanisms. — Evol. Dev. 2: 49-57.

Arthur, W. (2004). Biased embryos and evolution. — Cambridge University Press, Cambridge.

Atchley, W.R. & Hall, B.K. (1991). A model for development and evolution of complex morphological structures. — Biol. Rev. 66: 101-157.

Bell, M.A. & Foster, S.A., eds (1994). The evolutionary biology of the threespine stickleback. — Oxford University Press, Oxford.

Bell, M.A., Aguirre, W.E. & Buck, N.J. (2004). Twelve years of contemporary armor evolution in a threespine stickleback population. — Evol. Int. J. Org. Evol. 58: 814-824.

Bookstein, F.L. (1997). Landmark methods for forms without landmarks: morphometrics of group differences in outline shape. — Med. Imag. Anal. 1: 225-243.

Caldecutt, W.J. & Adams, D.C. (1998). Morphometrics of trophic osteology in the threespine stickleback, *Gasterosteus aculeatus.* — Copeia: 827-838.

Colosimo, P.F., Peichel, C.L., Nereng, K., Blackman, B.K., Shapiro, M.D., Schluter, D. & Kingsley, D.M. (2004). Genetic architecture of parallel armor plate reduction in threespine sticklebacks. — Publ. Libr. Sci. Biol. 2: E109.

Colosimo, P.F., Hosemann, K.E., Balabhadra, S., Villarreal Jr., G., Dickson, M., Grimwood, J., Schmutz, J., Myers, R.M., Schluter, D. & Kingsley, D.M. (2005). Widespread parallel evolution in sticklebacks by repeated fixation of ectodysplasin alleles. — Science 307: 1928-1933.

Cresko, W.A., Amores, A., Wilson, C., Murphy, J., Currey, M., Phillips, P., Bell, M.A., Kimmel, C.B. & Postlethwait, J.H. (2004). Parallel genetic basis for repeated evolution of armor loss in Alaskan threespine stickleback populations. — Proc. Natl. Acad. Sci. USA 101: 6050-6055.

Cresko, W.A., McGuigan, K.L., Phillips, P.C. & Postlethwait, J.H. (2007). Studies of threespine stickleback developmental evolution: progress and promise. — Genetica 129: 105-126.

Godfrey, L.R. & Sutherland, M.R. (1995). What's growth got to do with it? Process and product in the evolution of ontogeny. — J. Human Evol. 29: 405-431.

Gould, S.J. (1977). Ontogeny and phylogeny. — Belknap Press of Harvard University Press, Cambridge, MA.

Guralnick, R. & Kurplus, J. (2001). Spatial and temporal growth patterns in the phenotypically variable *Littorina saxatilis*: surprising patterns emerge from chaos. — In: Beyond heterochrony: the evolution of development (Zelditch, M.L., ed.). John Wiley & Sons, New York, NY, p. 195-228.

Hughes, G.M. (1960). A comparative study of gill ventilation in marine teleosts. — J. Exp. Biol. 37: 11-27.

Kimmel, C.B., Ullmann, B., Walker, M.B., Miller, C.T. & Crump, J.G. (2003). Endothelin1-mediated regulation of pharyngeal bone development in zebrafish. — Development 130: 1339-1351.

Kimmel, C.B., Walker, M.B. & Miller, C.T. (2007). Morphing the hyomandibular skeleton in development and evolution. — J. Exp Zool. (Mol. Dev. Evol.) 308B, 609-624.

Kimmel, C., Ullmann, B., Walker, C., Wilson, C., Currey, M., Phillips, P.C., Bell, M.A., Postlethwait, J.H. & Cresko, W.A. (2005). Evolution and development of facial bone morphology in threespine sticklebacks. — Proc. Natl. Acad. Sci. USA 102: 5791-5796.

Klingenberg, C.P. (1998). Heterochrony and allometry: the analysis of evolutionary change in ontogeny. — Biol. Rev. 73: 79-123.

Lauder, G. (1979). Feeding mechanics in primitive teleosts and in the halecomorph fish *Amia calva*. — J. Zool. 187: 543-578.

Lauder, G. & Liem, K. (1983). The evolution and interrelationships of the actinopterygian fishes. — Bull. Mus. Comp. Zool. 150: 95-197.

McKinney, M.L. & McNamara, K.J. (1991). Heterochrony: the evolution of ontogeny. — Plenum Press, New York, NY.

McKinnon, J.S. & Rundle, H.D. (2002). Speciation in nature: the threespine stickleback model systems. — Trends Ecol. Evol. 17: 480-488.

Miller, C.T., Swartz, M.E., Khuu, P.A., Walker, M.B., Eberhart, J.K. & Kimmel, C.B. (2007). *mef2ca* is required in cranial neural crest to effect Endothelin1 signaling in zebrafish. — Dev. Biol. 308: 144-147.

Peichel, C.L. (2005). Fishing for the secrets of vertebrate evolution in threespine sticklebacks. — Dev. Dyn. 234: 815-823.

Raff, R.A. (1996). The shape of life: genes, development, and the evolution of animal form. — University of Chicago Press, Chicago, IL.

Rohlf, F.J. (1998). On applications of geometric morphometrics to studies of ontogeny and phylogeny. — Syst. Biol. 47: 147-158.

Rohlf, F.J. (2004). tps Thin-plate spline version 1.20. — Department of Ecology and Evolution, State University of New York, Stony Brook, NY.

Rohlf, F.J. (2005a). tps Dig version 2.04. — Department of Ecology and Evolution, State University of New York, Stony Brook, NY.

Rohlf, F.J. (2005b). tps Regress, version 1.31. — Department of Ecology and Evolution, State University of New York at Stony Brook.

Rohlf, F.J. (2005c). tps Relative warps version 1.42. — Department of Ecology and Evolution, State University of New York, Stony Brook, NY.

Shapiro, M.D., Marks, M.E., Peichel, C.L., Blackman, B.K., Nereng, K.S., Jonsson, B., Schluter, D. & Kingsley, D.M. (2004). Genetic and developmental basis of evolutionary pelvic reduction in threespine sticklebacks. — Nature 428: 717-723.

Schlichting, C.D. & Pigliucci, M. (1998). Phenotypic evolution: a reaction norm perspective. — Sinauer Associates, Sunderland, MA.

Schluter, D. (2000). The ecology of adaptive radiations. — Oxford University Press, Oxford.

Smolyar, I.V. & Bromage, T.G. (2004). Discrete model of fish scale incremental pattern: a formalization of the 2D anisotropic structure. — ICES J. Mar. Sci. 61: 992-1003.

Thompson, D.W. (1942). On growth and form: a new edition. — Cambridge University Press, Cambridge.

Walker, J.A. (1997). Ecological morphology of lacustrine threespine stickleback *Gasterosteus aculeatus* L. (Gasterosteidae) body shape. — Biol. J. Linn. Soc. 61: 3-50.

Walker, J.A. & Bell, M.A. (2000). Net evolutionary trajectories of body shape evolution within a microgeographic radiation of threespine sticklebacks. — J. Zool. Lond. 252: 293-302.

Zelditch, M.L., ed. (2001). Beyond heterochrony: the evolution of development. — John Wiley & Sons, New York, NY.

Zelditch, M.L., Sheets, H.D. & Fink, W.L. (2000). Spatiotemporal reorganization of growth rates in the evolution of ontogeny. — Evolution 54: 1363-1371.

Zelditch, M.L., Swiderski, D.L., Sheets, H.D. & Fink, W.L. (2004). Geometric morphometrics for biologists: a primer. — Elsevier Science, Amsterdam.